

COHERENCE IN HIGH TEMPERATURE SUPERCONDUCTORS

Editors

**GUY DEUTSCHER
ALEX REVCOLEVSCHI**

World Scientific

DEUTSCHER
REVCOLEVSCHI

COHERENCE IN HIGH TEMPERATURE
SUPERCONDUCTORS



ISBN 981-02-2650-0

reduction in the bulk contribution, again consistent with a large local perturbation by the Zn.

17. N. Momono, M. Ido, T. Nakano, M. Oda, Y. Okajima and K. Yamaya, *Physica C* **233** (1994) 395
18. A.V. Mahajan, H. Alloul, G. Collin, J.F. Marucco, *Phys. Rev. Lett.* **72** (1994) 3100
19. G.-Q. Zheng, T. Kuse, Y. Kitaoka, S. Ohsugi, K. Asayama and Y. Yamada, *Physica C* **208** (1993) 339
S. Ohsugi, Y. Kitaoka, K. Ishida, S. Matumoto and K. Asayama, *Physica B* **186-188** (1993) 1027
20. P. Mendels, H. Alloul, G. Collin, N. Blanchard, J.F. Marucco and J. Bobroff, *Physica C* **235-240** (1994) 1595
21. P.W. Anderson, "Localized Moments" in *Many-Body Physics* (Cecil DeWitt Ed., Gordon and Breach, New York, London, Paris, 1967);
P.-G. de Gennes, *Superconductivity of Metals and Alloys* (Benjamin, New York, 1966), p.264
P.G.de Gennes and G.Sarma, *J.Appl.Phys.* **34** (1963) 1380
22. N. Ishikawa, N.Kuroda, H. Ikeda and R. Yoshizaki, *Physica C* **203** (1992) 284

ELECTRONIC STRUCTURE AND HIGH T_c SUPERCONDUCTIVITY : AN ITINERANT ELECTRON APPROACH

J. BOK, J. BOUVIER and L. FORCE
Laboratoire de Physique du Solide, CNRS-ESPCI,
10, rue Vauquelin 75231 PARIS cedex 05. FRANCE.
E-mail bok@hugo.espci.fr

ABSTRACT

We use an itinerant electron approach to describe the physical properties of high T_c cuprates. This approach is justified by many recent photoemission experiments which show a metallic Fermi surface (F.S.) and the presence of van Hove singularities close to the Fermi level. Other experiments, such as inelastic neutron scattering show that antiferromagnetic correlations disappear or become very weak in samples where T_c is maximum.

We review the van Hove scenario, which explains high T_c, anomalous isotope effects, low values of the coherence length, NMR Knight shift of ⁷Li. We take into account the Coulomb repulsion and show that a weakly screened electron-phonon interaction explains the observed gap anisotropy.

1. Introduction

It is now well accepted that the origin of cuprate superconductivity is to be found in the CuO₂ planes which are weakly coupled together in the c direction, so that their electronic properties are nearly two dimensional. For low oxygen content (no doping) all copper ions in this plane are Cu⁺⁺ ions, the material is an antiferromagnetic insulator due to strong electron-electron repulsion on the same copper site. With additional oxygenation or doping, holes are introduced in the CuO₂ planes and the compound becomes conducting and superconducting for T < T_c. The maximum T_c is achieved when the hole content is around 16 % per Cu atom. The physical mechanism leading to high T_c superconductivity in the cuprates is still controversial. One of the main questions is the following : are electron-electron correlations still dominant for 16 % doping¹, or is an itinerant electron approach valid² ? In this paper we shall review the itinerant electron model and compare its results with experiments.

Many recent experimental results are in favour of this Fermi liquid approach. Angular resolved photoemission spectroscopy (ARPES) has been performed by three different groups in Stanford³, Argonne⁴ and Wisconsin⁵ in five different compounds Bi₂Sr₂CuO₆ (Bi 2201), Bi₂Sr₂CaCu₂O₈ (Bi 2212), YBa₂Cu₃O₇ (Y123), YBa₂Cu₄O₈

(Y124) and $\text{Nd}_{2-x}\text{Ce}_x\text{CuO}_{4+\delta}$ (NCCO). The general result is that, in the normal state, all these compounds show metallic-like Fermi surfaces (F.S.) (large F.S. occupying the major part of the area of the Brillouin zone). For small doping, the F.S. is composed of small hole pockets. All these findings agree well with band structure calculations⁶, i.e. an itinerant electron model.

On the other hand, inelastic neutron scattering shows strong antiferromagnetic (A.F.) correlations⁷ in $\text{YBa}_2\text{Cu}_3\text{O}_{6+x}$ for $x < 0.7$. However, when x varies between 0.9 and 1, the A.F. correlation length ξ_a decreases strongly in the superconducting states and $\xi_a/a \sim 1$ for $x = 1$, a is the lattice parameter. The intensity of magnetic contributions in the normal state also decreases strongly⁸. The normal state pseudogap in the excitations has also been probed by various experimental techniques : N.M.R., transport and μSR ⁹. All these experiments show that the pseudogap goes to zero for optimal doping (corresponding to maximum T_c). It is difficult to imagine that antiferromagnetic correlations (A.F.C.) are responsible for superconductivity in the cuprates, and that these A.F.C. disappear or become very weak when T_c is maximum.

In this paper we shall review what we call the van Hove scenario, i.e. an itinerant electron model with the additional assumption that the Fermi level lies close to a v.H. singularity (v.H.s.) when T_c is high. We shall review 1) the band structure of the cuprates, 2) the calculation of T_c in the framework of the v.H. scenario^{2,10} and its consequences, 3) we shall take into account the Coulomb repulsion between electrons and show that renormalization effects still exist in wide bands¹¹, 4) we compute the coherence length and show that we obtain the correct value, 15\AA , using experimentally determined parameters, 5) we show that the measured Knight shift in the nuclear magnetic resonance of ^7Li in YBaCuO can be explained by a logarithmic density of states and finally 6) we explain the observed gap anisotropy using a weakly screened electron-phonon interaction.

2. Band Structure of the Cuprates

The simplest band structure we can take for a square lattice is

$$\varepsilon_k = -2t(\cos k_x a + \cos k_y a) \quad (2.1)$$

where t is an interaction with nearest neighbours; this gives a square Fermi surface, and the v.H.s. corresponds to half filling (figure 2-1). We know that this is not a good representation of the high T_c cuprates because, for half filling (one electron per copper site), they are antiferromagnetic insulators. We think that the Fermi level is at the v.H.s. for the doping corresponding to maximum T_c , i.e. 16 % of holes per Cu in each CuO_2 plane or 0.42 filling of the first Brillouin zone (B.Z.). This can be achieved by taking into account the repulsive interaction between second nearest neighbours and the effect of the rhomboedric distortion¹².

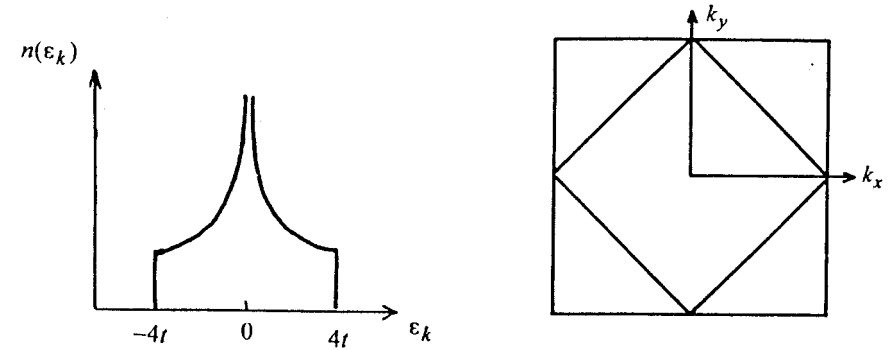


Fig. 2-1 : Density of states $n(\varepsilon)$ and Fermi surface for a band given by Eq. (2.1).

With the repulsive interaction with second nearest neighbours (s.n.n.), the band structure becomes:

$$\varepsilon_{\vec{k}} = -2t(\cos k_x a + \cos k_y a) + 4\alpha t \cos k_x a \cos k_y a \quad (2.2)$$

where αt is an integral representing the interaction with s.n.n.. The singularity occurs for $\varepsilon = -4\alpha t$, i.e. there is a shift towards lower energy. The Fermi surface at the v.H.s. is no longer a square but is rather diamond-shaped (figure 2-2). For $\alpha = 0.1$, this corresponds to a 46 % filling of the B.Z.

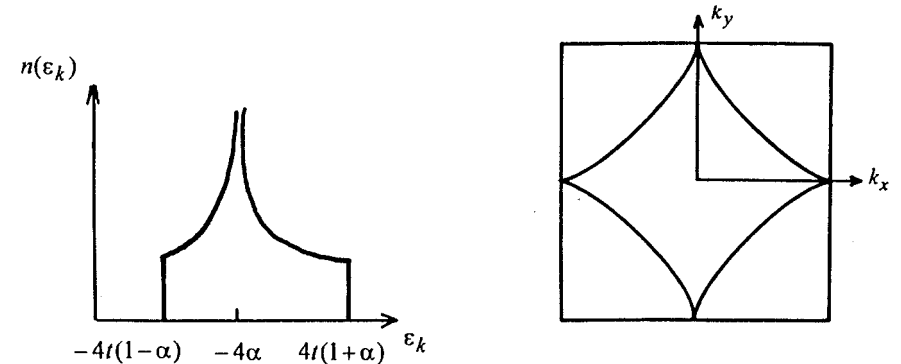


Fig. 2-2 : Density of states $n(\varepsilon)$ and Fermi surface for a band given by Eq. (2.2).

With a rhomboedric distortion, the band structure is then

$$\epsilon_{\vec{k}} = -2t(1 + \beta) \cos k_x a - 2t \cos k_y a \quad (2.3)$$

where βt represents the difference in the interaction with first neighbours in the x and y directions. The effect is now that the singularity is split in two (figure 2-3).

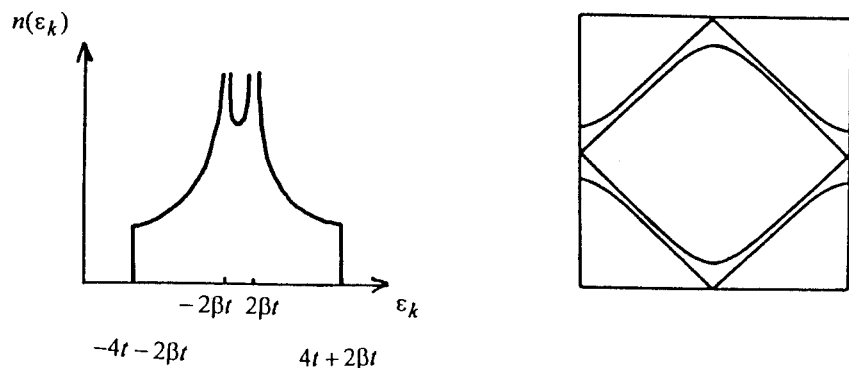


Fig. 2-3 : Density of states $n(\epsilon)$ and Fermi surface for a band given by Eq. (2.3).

We may combine both effects and, with $\alpha = 0.1$ and $\beta = 0.1$, the first singularity is at 41 % of filling and the second at 51 % (figure 2-4). The second one has no physical meaning because near half filling electron-electron interaction opens a gap. Superconductivity is observed only when the Fermi level lies in the vicinity of the first v.H.s..

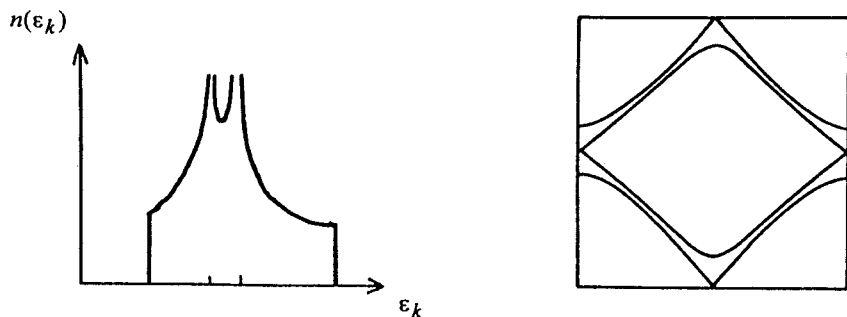


Fig. 2-4 : Density of states $n(\epsilon)$ for a band given by Eq. (2.2) and (2.3) with $\alpha = 0.1$ and $\beta = 0.1$.

Many more elaborate band structure calculations have been done for the cuprates^{12,13}. Most of them confirm the two dimensional character of the electronic structure of these compounds in the CuO_2 planes. They all find saddle points with singularities in the D.O.S. more or less near the Fermi level. A recent calculation of the band structure of the mercury cuprates¹⁴ finds the Fermi level exactly pinned at the v.H.s. for the doping corresponding to the maximum T_c , thus confirming our simple model.

Recently, several experiments have been reported that measure the properties of the Fermi surface in the high T_c cuprates, especially for Bi 2122^{3,5} and YBaCuO 1237 and 1248^{4,15}. The technique used is angle-resolved photoemission spectroscopy (ARPES), which requires a careful preparation of the surface. All the results which were obtained confirm the existence of a v.H.s. (or flat band, or saddle point) at the Fermi level for optimum doping. We present in figure 2-5 the results obtained by Dessau et al¹⁶ for Bi 2122. Figure 2-5 represents the energy of the electron measured from the Fermi level versus \vec{k} for three directions in the Brillouin zone $\Gamma Y, Y\bar{M}$ and $\bar{M}\Gamma$. A square B.Z. is used : Y is the center of the square, Γ the corner and M the middle of a side. Measurements are made only near regions A and B. Region A corresponds to the maximum of Fermi velocity. From the experimental results we find $v_{F\text{max}} = 3.10^7$ cm/s. Region B corresponds to the v.H.s. and to a zero Fermi velocity. For comparison we put the curve representative of formula (2.1) on the same figure (in small dots). We see that the experimental band is flatter than that given by Eq. (2.1), but we take our formula (2.1) as a first approximation. By comparison with experiment, we find $t = 0.20$ eV or 0.25 eV and for the band width $W = 8t = 1.6$ or 2 eV.

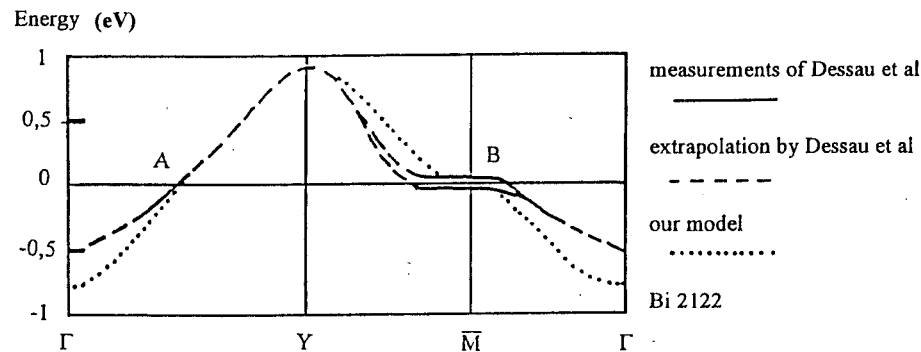


Fig.2-5 : Energy of the electrons measured from the Fermi level versus \vec{k} for three directions in the Brillouin zone.

Density of states (D.O.S.)

We know that near the v.H.s. the D.O.S. is logarithmic

$$n(\varepsilon) = n_1 \ln \left| \frac{D^*}{\varepsilon} \right| \quad (2.4)$$

in which the values of D^* and n_1 are determined from the band structure. From the simple model given by Eq. (2.2), we find¹⁷:

$$n_1 = 8/(\pi^2 D^*) \text{ per spin, per unit cell,}$$

and

$D^* = 16 t \sqrt{1 - \alpha^2/4}$. We remark that D^* is larger than the band width $8t$. We know that whatever the exact band structure in 2D, the DOS is constant near the band edges ($\pm W/2$) and logarithmic near the v.H.s.. We shall thus take the following approximation:

- a constant D.O.S. n_0 between $-W/2$ and $+W/2$,

- a logarithmic peak $n = n_1 \ln \left| \frac{D}{\varepsilon} \right|$ between $-D$ and $+D$.

Near the v.H.s. this is equivalent to formula (2.4) with $D^* = D \exp(n_0/n_1)$. The constants D , n_0 and n_1 are not independent. The total number of states in the band is fixed. We have one orbital state (i.e. two spin states) per copper atom so that

$$n_0 W + 2n_1 D = 1$$

n_0 is also given by the effective mass at the band edge.

For example, for $W = 2\text{eV}$ ($t = 0.25\text{eV}$), we obtain $n_0 = 0.3\text{ states/eV/Cu atom}$ and $n_1 = 0.2$ which gives $D = 0.9\text{ eV}$. We shall also make calculations with $D = 0.3\text{ eV}$, corresponding to a much narrower v.H.s., as observed experimentally.

3. The Labbé-Bok Formula

This formula was obtained² using the following assumptions:

1- The Fermi level lies at the van Hove singularity,

2- The B.C.S. approximations:

-The electron-phonon interaction is isotropic and so is the superconducting gap Δ .

-The attractive interaction V_p between electrons is non-zero only in an interval of energy $\pm \hbar\omega_0$ around the Fermi level where it is constant. When this attraction is mediated by emission and absorption of phonons, ω_0 is a typical phonon frequency.

In that case, the critical temperature is given by:

$$k_B T_c = 1.13 D \exp \left[-\sqrt{\frac{1}{\lambda} + \ln^2 \left(\frac{\hbar\omega_0}{D} \right)} - 1.3 \right] \quad (3.1)$$

where $\lambda = n_1 V_p / 2$.

A simplified version of formula (3.1), when $\hbar\omega_0$ is not too small compared to D , is:

$$k_B T_c = 1.13 D \exp(-1/\sqrt{\lambda})$$

The two main effects enhancing T_c are:

- 1- The prefactor in formula (3.1) is an electronic energy much larger than a typical phonon energy ω_0 .
- 2- λ is replaced by $\sqrt{\lambda}$ in formula (3.1). In the weak coupling limit, when $\lambda < 1$, the critical temperature given by formula (3.1) is very high. In fact it gives too high values of T_c . We shall see later that this is due to the fact that we have neglected Coulomb repulsion between electrons. Taking this repulsion into account, we shall obtain values for T_c which are very close to the observed ones.

As it is however, this approach already explains many of the properties of the high T_c cuprates near optimum doping.

- The variation of T_c with doping. The highest T_c is obtained when the Fermi level is exactly at the v.H.s.. For lower or higher doping, the critical temperature decreases. That is what is observed experimentally¹⁸.
- The isotope effect. Labbé and Bok² showed using formula (3.1), that the isotope effect is strongly reduced for high T_c cuprates. C.C. Tsuei et al¹⁹ have calculated the variation of the isotope effect with doping and shown that it explains the experimental observations (figure 3-1).

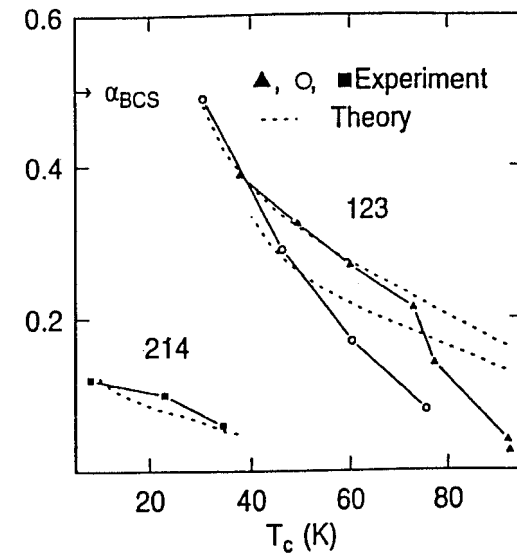


Fig. 3-1: Isotopic effect in La_2CuO_4 (214) and YBaCuO (123).

- Marginal Fermi liquid behaviour :

In a classical Fermi liquid, the lifetime broadening $1/\tau$ of an excited quasi-particle goes as ϵ^2 . The marginal Fermi liquid situation is the case where $1/\tau$ goes as ϵ . Theoretically, marginal behaviour has been established in two situations : (a) for the half-filled nearest-neighbour coupled Hubbard model on a square lattice and (b) when the Fermi level lies at a v.H. singularity¹⁹. Experimental evidence of marginal Fermi liquid behaviour has been seen in angle-resolved photoemission²⁰, infrared data²¹ and temperature dependence of electrical resistivity²². Marginal Fermi liquid theory, in the framework of v.H.s. predicts a resistivity linear with temperature T . This was observed by Kubo et al²². They also observe that the temperature dependence of the resistivity goes from T , for a high T_c material to T^2 as the system is doped away from the T_c maximum, which is consistent with our picture; in lower T_c material, the Fermi level is pushed away from the singularity (figure 3-2).

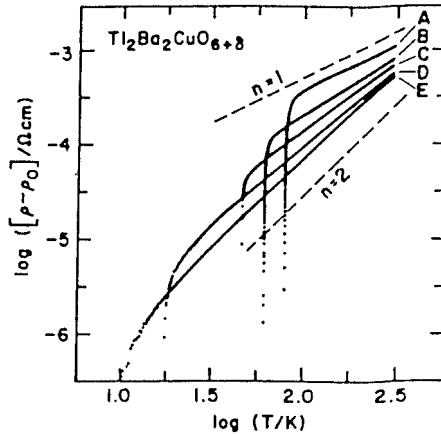


Fig. 3-2 : Resistivity ρ versus temperature. For the highest T_c compounds ρ varies linearly with T ; for low T_c compounds, the variation is quadratic, from ref [22].

4. The Coulomb Repulsion between Electrons

As early as 1962, Anderson and Morel²³ have shown that the electron-electron repulsion plays a central role in superconductivity. Assuming a constant repulsive potential $V_{kk'} = V_c$ from 0 to E_F , they find that T_c is given by :

$$T_c \cong T_0 \exp \left[-\frac{1}{\lambda - \mu^*} \right] \quad (4.1)$$

$$\text{with } \mu = N_0 V_c \quad \text{and} \quad \mu^* = \frac{\mu}{1 + \mu \ln(E_F / \omega_0)}$$

M.L. Cohen and P. W. Anderson²⁴ assumed that for stability reasons μ is always greater than λ . V. Ginzburg²⁵ gave arguments that in some special circumstances μ can be smaller than λ . Nevertheless, if we take $\mu \geq \lambda$, superconductivity only exists because μ^* is of the order of $\mu/3$ to $\mu/5$ for a Fermi energy of the order of $100 \omega_0$. It is useless to reduce the width of the band W ($E_F = W/2$ for a half-filled band) because λ and μ vary simultaneously and μ^* becomes greater if E_F is reduced, thus giving a lower T_c . Superconductivity can even disappear in a very narrow band if $\lambda - \mu^*$ becomes negative.

We have shown¹¹ that, nevertheless, high T_c can be achieved in a metal containing almost free electrons (Fermi liquid) in a broad band, with a peak in the D.O.S. near the middle of the band.

Taking a D.O.S., equal to a constant n_0 between energies $-W/2$ and $+W/2$, (the zero of energy is at the Fermi level) with the additional singularity $n(\epsilon) = n_1 \ln |D^* / \epsilon| + n_0$ between $-D$ and $+D$ we find for T_c , the following formula :

$$k_B T_c = \frac{D}{2} \exp \left[0.819 + \frac{n_0}{n_1} - \sqrt{F} \right] \quad (4.2)$$

where

$$F = \left(\frac{n_0}{n_1} + 0.819 \right)^2 + \left(\ln \frac{\hbar \omega_0}{D} \right)^2 - 2 - \frac{2}{n_1} \left(n_0 \ln \frac{2.28 \hbar \omega_0}{D} - \frac{1}{V_p - V_c^*} \right)$$

$$V_c^* = \frac{V_c}{1 + V_c \left[\frac{n_1}{2} \left(\ln \frac{D}{\hbar \omega_0} \right)^2 + n_0 \ln \frac{W}{2 \hbar \omega_0} \right]}$$

We can have a few limiting cases for this formula :

- 1) $n_1 = 0$: no singularity. We find the Anderson-Morel formula.
- 2) $V_c = 0$ and $n_0 = 0$: this gives the Labbé-Bok formula.

There are many effects enhancing T_c :

$\lambda - \mu^*$ is reduced by the square root, down to $\sqrt{\lambda_1 - \mu_1^*}$ when n_1 is large enough. As $\lambda - \mu^* < 1$, the critical temperature is strongly increased because this factor appears in an exponential.

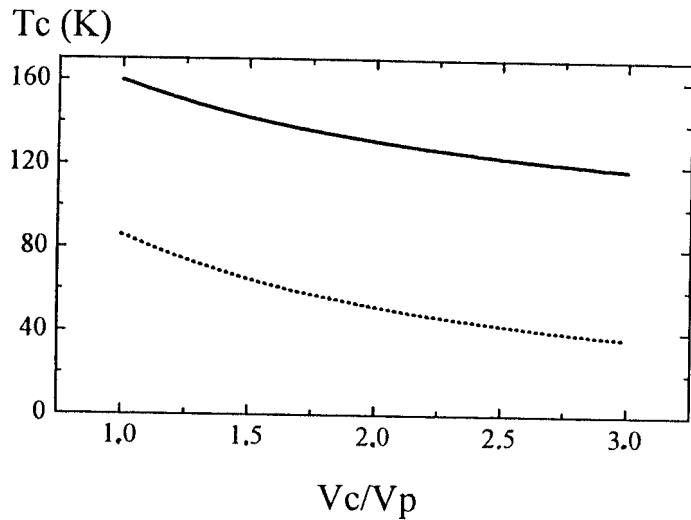


Fig. 4-1 : Effect of Coulomb repulsion on T_c . The following numerical values have been used :
 (solid line) $D = 0.9$ eV, $n_0 = 0.3$ states/eV/Cu atom, $W = 2$ eV, $n_1 = 0.2$.
 (dotted line) $D = 0.3$ eV, $n_0 = 0.3$ states/eV/Cu atom, $W = 3$ eV, $n_1 = 0.16$.

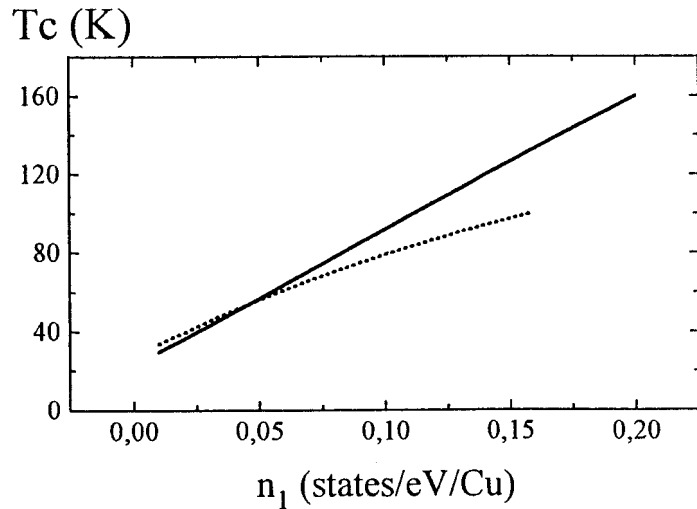


Fig. 4-2 : Influence of the number of electrons in the singularity n_1 , on the critical temperature T_c . The numerical values are the same as in figure 4-1, and with $n_0 = (1 - 2n_1) / W$, and $V_c = V_p$.

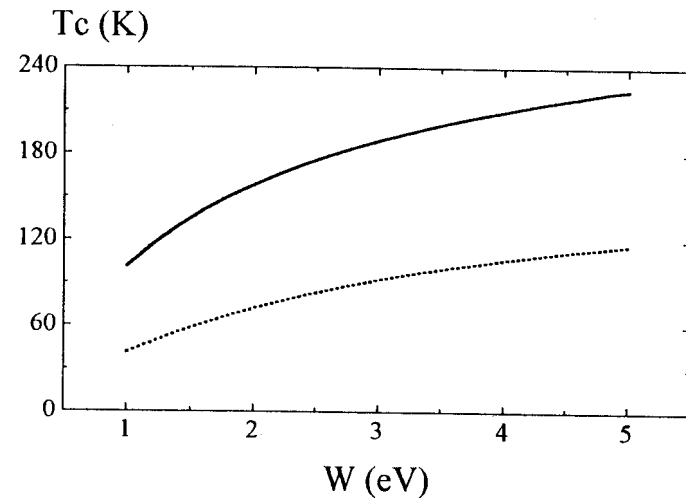


Fig. 4-3 : Influence of the band width W on T_c . The numerical values are :
 (solid line) $D = 0.44/W$, $n_0 = 0.6/W$, $n_1 = 0.4/W$, $V_p = W/2$ and $V_c = V_p$,
 (dotted line) $D = 0.3$ eV, $n_0 = 0.9/W$, $n_1 = 0.05/D$, and $V_c = V_p$.

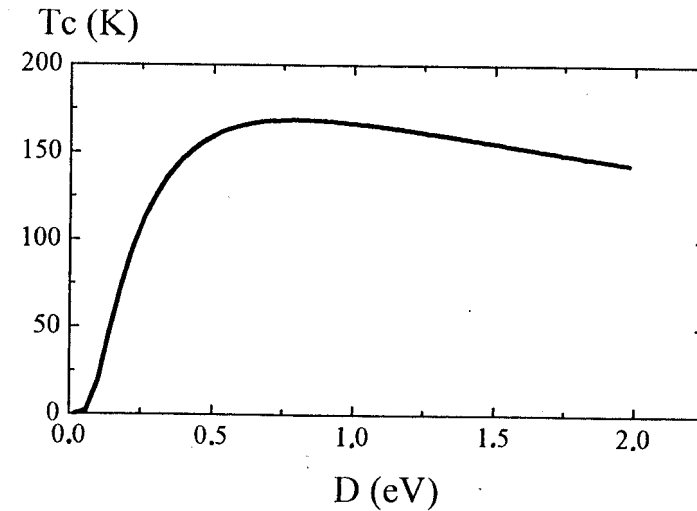


Fig. 4-4 : Effect of the width of the singularity D on T_c . n_0 and the total number of electrons per unit cell are maintained constant with this set of parameters.
 Then $W = 2$ eV, $n_0 = 0.3$ eV/states/Cu, $n_1 = 0.2/D$.
 In all these cases the calculation are made so that the total number of states of the band is one by Cu atom.
 Then $n_0 W + 2 n_1 D = 1$, and $\lambda = (n_0 + n_1) V_p$. In all these cases $\hbar\omega_0 = 0.05$ eV and $\lambda = 0.5$.

The prefactor before the exponential is the singularity width D , instead of $\hbar\omega_0$. We expect $D > \hbar\omega_0$. For instance D may be of the order of 0.5 eV and ω_0 about a few 10 meV ($D/\hbar\omega_0$ of the order of 5 to 10).

We have made some numerical calculations using formula (4.2) to illustrate the effect of Coulomb repulsion. We used two values of D : $D = 0.9$ eV corresponding to $t = 0.25$ eV and a much smaller value $D = 0.3$ eV. These calculations are illustrated by figures 4-1 to 4-4.

These calculations show that the Coulomb repulsion does not kill superconductivity in the framework of the Labbé-Bok (L.B.) model. The general rule for high T_c in this model is to have a peak in the density of states near the middle of a broad band to renormalize the effective repulsion μ .

5. Coherence Length and Anisotropy Effects

The relation between the Fermi velocity v_F and the intrinsic coherence length ξ_0 is, in the framework of the B.C.S. theory, $\xi_0 = \hbar v_F / \pi \Delta$. This is valid for a spherical Fermi surface where v_F is constant.

If we take for v_F , the maximum value measured by Dessau et al, $v_F = 3.10^7$ cm/s, we find with the B.C.S. formula $\xi_0 = 30$ Å while the experimental value is between 10 and 15 Å. Actually, these calculations do not take into account the fact that the singular points corresponding to $v_F = 0$ have an important statistical weight. The density of states is given by :

$$n(\epsilon)d\epsilon = \int_{\Gamma} \frac{dk_{\parallel} dk_{\perp}}{2\pi^2}$$

where Γ is a constant energy surface and dk_{\parallel} and dk_{\perp} are the tangential and orthogonal components of dk . If, following B.C.S., we construct a wave packet of width 2Δ , the average Fermi velocity becomes :

$$\hbar\bar{v}_F = \frac{2\Delta \int_{\Gamma} dk_{\parallel}}{2\pi^2 \int_{-\Delta}^{+\Delta} n(\epsilon)d\epsilon}$$

with the energy band given by Eq. (2.1) and the Fermi level at the singularity, we find :

$$\hbar\bar{v}_F = \frac{2\sqrt{2} \pi \alpha t}{1 + \ln(16t/\Delta)}$$

or

$$\bar{v}_F = \frac{\pi v_{F\max}}{1 + \ln(16t/\Delta)} \quad (5.1)$$

In formula (5.1) all parameters $v_{F\max}$, t and Δ have been measured experimentally; with the following numerical values, $v_{F\max} = 3.10^7$ cm/s, $8t = 1.5$ eV, $\Delta = 20$ meV, we find $\bar{v}_F = 1.5 \cdot 10^7$ cm/s and $\xi_0 = 15$ Å. We insist that this observed value is obtained without any adjustable parameter.

G. Deutscher et al²⁶ measured by point contact spectroscopy a value of v_F which is twice the value that we used. They attribute the difference obtained in these two experiments to renormalization effects due to electron-phonon and electron-electron coupling. These renormalization effects are discussed in a recent paper by G. Deutscher and P. Nozières²⁷.

6. Magnetic Susceptibility and Knight Shift of ⁷Li in YBCO

Bok and Labbé, using their model², have also predicted that the magnetic susceptibility of itinerant electrons follows a logarithmic law versus temperature²⁸ :

$$\chi_{i.e.}(T) = \frac{8\mu_0 \mu_B^2}{\pi^2 D^*} \left(\ln \frac{D^*}{2k_B T} + \frac{\pi^2}{12} \right) \quad (6.1)$$

where $\mu_0 = 4\pi \cdot 10^{-7}$ in SI units, and μ_B is the Bohr magneton.

Recently K. Sauv et al^{29,30} have measured the Knight shift ΔK of the ⁷Li RMN line in Li-doped YBaCuO, and have observed the law :

$$\Delta K = \alpha \chi_{ie}(T) + \beta \chi_0 = a \ln \frac{1}{T} + b \quad (6.2)$$

where χ_0 represents the other contributions to the magnetic susceptibility which are temperature independent (core electrons, diamagnetic contributions, etc); α and β are given by :

$$\alpha = \frac{1}{\mu_B} H_{eff}^{(0)} \quad \text{and} \quad \beta = \frac{1}{\mu_B} H_{eff}^{(1)}$$

where $H_{eff}^{(0,1)}$ is the hyperfine field experienced by the Li nucleus.

Here the Li atom is assumed to be located in the CuO₂ planes and, so, can play the role of a local probe for the 2D itinerant electrons in these planes.

K. Sauv et al, have studied the RMN Knight shift for several low doping x of Li, with x between 0.0062 and 0.019, with no change in the oxygen concentration of 7.01 ± 0.02 . Then we can calculate a relative equivalent shift of the Fermi level from the singularity³¹ :

$$\delta = \frac{E_F - E_s}{k_B T} \quad (6.3)$$

for each value of x , and determine the variation of ΔK or $\chi_{i.e.}(T)$ with the following formula:

$$\chi_{ie}(T) = \frac{1}{2} \frac{\mu_0 \mu_B}{B} k_B T \sinh u \frac{8}{\pi^2 D^*} \left[I_1 \ln \frac{D^*}{k_B T} + I_2 \right] \quad (6.4)$$

$$\text{where } I_1 = \int_{-\infty}^{+\infty} \frac{1}{\cosh y' + \cosh u} dy', \quad I_2 = - \int_{-\infty}^{+\infty} \frac{\ln|y|}{\cosh y' + \cosh u} dy'$$

$$\text{with } u = \frac{\mu_B B}{k_B T} \ll 1, \quad y = \frac{E}{k_B T}, \quad y' = y - \delta$$

and where B is the applied magnetic field^{29,30}.

Like in the experimental results we find that in this range value of x, neither the slope a, nor the ordinate at the origin b vary, cf figure 6-1. Moreover, the slope a is fitted without adjustable parameters. The width of the singularity D^* comes from the ARPES measurements³²; and from Eq. (6.2), we may also write :

$$\alpha = \frac{B_f}{\mu_0 \mu_B}$$

where B_f is the effective field acting on the nucleus Li; we obtain $B_f = 4.6$ Tesla in the range values usually found for the Li atom in various compounds³³.

Once more, we see that the existence of the v.H.s. explains the temperature logarithmic law of the magnetic susceptibility, observed experimentally.

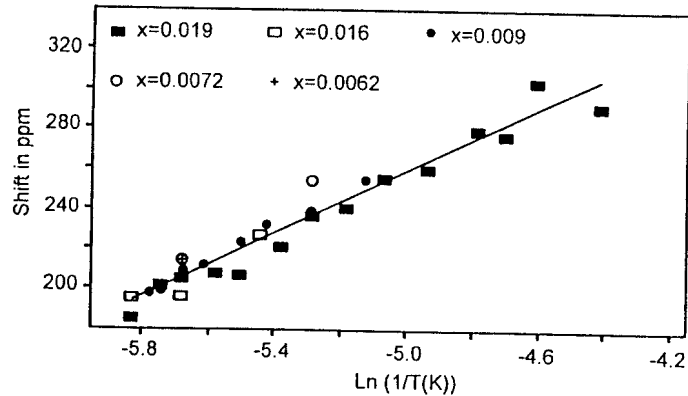


Fig. 6-1 : Variation of the Knight shift ΔK in ppm with $\ln(1/T)$.
Full line : calculation; symbol : experimental points.

7. Gap Anisotropy

We take a classical electron-electron interaction potential $V_{\vec{k}\vec{k}'}$ between two electron states of wave vector \vec{k} and \vec{k}' respectively, via electron-phonon coupling. From B.C.S.³⁴ this matrix element may be written :

$$V_{\vec{k}\vec{k}'} = \frac{|g_q|^2}{q^2 + q_0^2} \frac{(\hbar\omega_q)^2}{\epsilon_{\vec{k}\vec{k}'}^2 - (\hbar\omega_q)^2} \quad (7.1)$$

where $\vec{k}' - \vec{k} = \vec{q}$ is the phonon wave vector, $|g_q|^2$ is the square of an electron-phonon interaction matrix element, $\epsilon_{\vec{k}\vec{k}'} = \epsilon_{\vec{k}} - \epsilon_{\vec{k}'}$ is the electron energy difference and ω_q is the phonon frequency; q_0 is a screening vector, q_0^{-1} is the screening length. In the cuprates, the important phonons are the optical ones, so we take the usual approximation, $\omega_q = \omega_0 = \text{constant}$.

The interaction between electrons is attractive $V_{\vec{k}\vec{k}'} < 0$, as long as the energy variation $|\epsilon_{\vec{k}\vec{k}'}|$ is less than $\hbar\omega_0$. In most models, the last term of Eq. (7.1) is taken as -1. In our case, this is even more justified since the important contributions to Δ will come from states of vector \vec{k} near the saddle points taken on the Fermi surface, that is for energy differences close to zero. A. A. Abrikosov³⁵ has used the same approximation.

We first solve the problem at zero temperature, $T = 0$ K ; in this case the B.C.S. equation giving the gap $\Delta_{\vec{k}}$ reads :

$$\Delta_{\vec{k}} = - \frac{1}{2} \sum_{\vec{k}'} \frac{V_{\vec{k}\vec{k}'} \Delta_{\vec{k}'}}{\sqrt{\epsilon_{\vec{k}\vec{k}'}^2 + \Delta_{\vec{k}'}}^2} \quad (7.2)$$

$$\text{with } V_{\vec{k}\vec{k}'} = - \frac{|g_q|^2}{q^2 + q_0^2} < 0 \quad \text{and} \quad -\hbar\omega_0 < \epsilon_{\vec{k}\vec{k}'} < +\hbar\omega_0$$

and Eq. (7.2) may be rewritten, replacing the sum by an integral :

$$\Delta_{\vec{k}} = - \frac{1}{2} \iint \frac{V_{\vec{k}\vec{k}'} \Delta_{\vec{k}'}}{\sqrt{\epsilon_{\vec{k}\vec{k}'}^2 + \Delta_{\vec{k}'}}^2} dk'_x dk'_y \quad (7.3)$$

It is useful to introduce tangential and normal coordinates dk_t and dk_{\perp} ; dk_t is tangential to the constant energy curve Γ and dk_{\perp} is normal to this curve, we obtain :

$$dk_t dk_{\perp} = \frac{dk_{\perp}}{d\epsilon} d\epsilon dk_t \quad (7.4a)$$

but

$$\hbar|v_{\vec{k}}| = \frac{d\varepsilon}{dk_{\perp}} \quad \text{so that}$$

$$\hbar \frac{dk_{\perp}}{d\varepsilon} = \frac{1}{|v_{\vec{k}}|} = \frac{\hbar}{2ta \sqrt{\sin^2 k_x a + \sin^2 k_y a}} \quad (7.4b)$$

for $\varepsilon = \text{constant}$ and Eq. (2.1)
we find

$$dk_t = \frac{\sqrt{2}}{2} \frac{dk_x}{\sin k_y a} \sqrt{\sin^2 k_x a + \sin^2 k_y a} \quad (7.4c)$$

and finally

$$\sin k_y a = \left[1 - \left(\frac{\varepsilon}{2t} - \cos k_x a \right)^2 \right]^{1/2} \quad (7.4d)$$

by combining Eq. (7.2), (7.3) and (7.4) we obtain for the gap :

$$\Delta_{\vec{k}} = \lambda_{\text{eff}} \int_0^{\hbar\omega_0} d\varepsilon \int_{\Gamma} \frac{dk'_x a}{\left[1 - \left(\frac{\varepsilon}{2t} - \cos k'_x a \right)^2 \right]^{1/2}} \frac{(q_0 a)^2}{(q a)^2 + (q_0 a)^2} \frac{\Delta_{\vec{k}'}}{\sqrt{\varepsilon_{\vec{k}'}^2 + \Delta_{\vec{k}'}^2}} \quad (7.5)$$

λ_{eff} is a numerical parameter with no dimension; it includes an effective interaction V , an average density of states $N/\pi^2 t$, and a renormalized Coulomb repulsion μ^* .

Eq. (7.5) is an integral equation which is not easy to solve. But we know from symmetry considerations, that $\Delta_{\vec{k}}$ will have a fourfold symmetry; we can expand it in a Fourier series of the form :

$$\Delta_{\vec{k}} = \Delta_0 + \Delta_1 \cos 4\Phi + \dots \quad (7.6)$$

where Φ is the angle between \vec{k}_x and \vec{k} .

We solve Eq. (7.5) by iteration, we first replace in the integral $\Delta_{\vec{k}}$ by its average value Δ_0 , then compute Δ_1 , introduce Δ_1 in the integral, etc.

We shall present here only the first two steps : calculation of Δ_0 and Δ_1 , a detailed calculation will be given in a forthcoming paper. To compute Δ_0 and Δ_1 , we use the following procedure. Let us first take $\vec{k}a$ at point A $(0, \pi)$ (see figure 7-1).

$$\Delta_A = \Delta_{\text{maximum}} = \Delta_0 + \Delta_1$$

then at point B $(\pi/2, \pi/2)$

$$\Delta_B = \Delta_{\text{minimum}} = \Delta_0 - \Delta_1$$

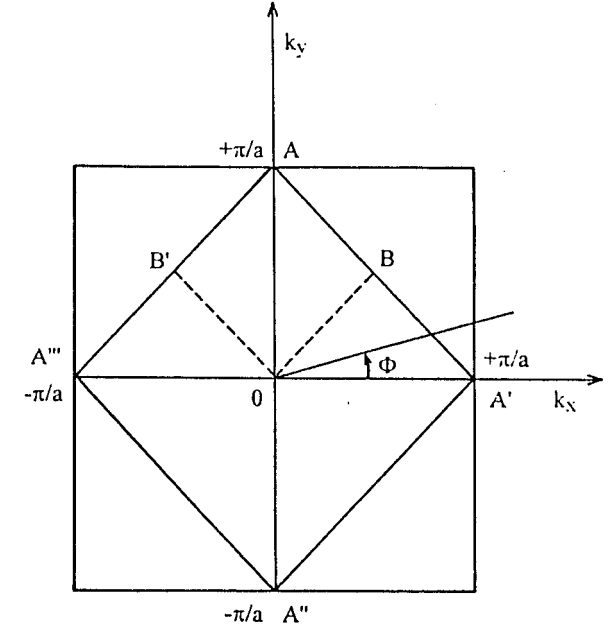


Fig. 7-1 : Square Fermi surface and the interesting points (A, A', B, B').

For Δ_A , the vector \vec{k}' must describe all the contour $AA'A''A'''$ but we see that this is twice the contour $AA'A''$. For large values of q , the integral is very small, so as a first approximation, we neglect large q values and integrate only from A to B and multiply by two; we thus obtain :

$$\Delta_{\text{max}} = \lambda_{\text{eff}} \int_0^{u_{\text{max}}} \frac{\Delta_0}{\sqrt{u^2 + u_0^2}} I_A(u) du \quad (7.7a)$$

$$\text{with } I_A(u) = \int_0^{\pi/2} \frac{dx'}{\left[1 - (u - \cos x')^2 \right]^{1/2}} \frac{2(q_0 a)^2}{2x'^2 + (q_0 a)^2} \quad (7.7b)$$

$$\Delta_{\text{min}} = \lambda_{\text{eff}} \int_0^{u_{\text{max}}} \frac{\Delta_0}{\sqrt{u^2 + u_0^2}} I_B(u) du \quad (7.8a)$$

$$\text{with } I_B(u) = \int_0^{x'} \frac{dx'}{\left[1 - (u - \cos x')^2\right]^{1/2}} \frac{2(q_0 a)^2}{2\left(x' - \frac{\pi}{2}\right)^2 + (q_0 a)^2} \quad (7.8b)$$

where $x' = k'_x a$, $x'_0 = \arccos(u/2)$, $u = \varepsilon/2t$, $u_0 = \Delta_0/2t$, $u_{\max} = \hbar\omega_0/2t$

λ_{eff} in these integrals is the isotropic part of the electron-phonon interaction; it is of the order of 0.5. These results allow a first qualitative comparison between Δ_{\max} and Δ_{\min} . In the integrals $I_A(u)$ and $I_B(u)$, the dominant contributions are those for which the velocity v_k goes to zero, i.e. the limit $x' \rightarrow 0$. We see that the multiplicative factor is 1 ($q = 0$) in the case of I_A and of the order of 1/6 to 1/7 in the other case ($q = \pi/2a$). We see that the physical origin of the gap anisotropy comes from the fact that, in certain directions, there are saddle points where $|v_k| \rightarrow 0$ and Δ_k is large and other directions for which $|v_k|$ is always finite and Δ_k is smaller. At finite temperature T , Eq. (7.7-7.8) are replaced by Eq. (7.9).

$$\Delta_{(\max,\min)} = \lambda_{\text{eff}} \int_0^{u_{\max}} \frac{\Delta_0(T)}{\sqrt{u^2 + u_0^2(T)}} I_{(A,B)}(u) \tanh\left(\frac{\sqrt{u^2 + u_0^2(T)}}{k_B T/t}\right) du \quad (7.9)$$

We evaluate numerically Δ_A and Δ_B using the two integral Eq. (7.7) and (7.8). To do that, we have to choose two parameters : the phonon frequency ω_0 and the transfer integral t . We could consider them as adjustable parameters to find the values of $\Delta_{\max} = 20 \pm 3 \text{ meV}$, $\Delta_{\min} = 5 \pm 5 \text{ meV}$ and $T_c = 86 \pm 2 \text{ K}$ observed experimentally^{4,36} for Bi 2212. For $\text{YBa}_2\text{Cu}_3\text{O}_{7-x}$ or $\text{YbBa}_2\text{Cu}_3\text{O}_{7-x}$ single crystals tunneling effects show a two-gap structure³⁷; with values for the maximum gap between 26 and 30 meV and for the minimum gap between 0.5 and 11 meV. Other recent tunneling spectroscopy measurements on Bi 2212³⁸ found $\Delta_{\max} = 29.5 \pm 4 \text{ meV}$ for $T_c = 92.3 \text{ K}$.

But, on the contrary, we have taken ω_0 and t from experimental measurements and we show that we obtain correct values for Δ and T_c . So our model contains no adjustable parameter, but leads to a low value of $q_0 a$; we discuss this point in the last part of this work.

The interaction term t has been estimated theoretically by band structure calculations⁶. We prefer experimental determinations. From ARPES measurements^{32,39} t is estimated to be between 0,20 and 0,25 eV.

For the choice of $\hbar\omega_0$, many authors have determined several frequencies of phonon modes which should play a major role in the superconductivity mechanism. The involved modes are mainly the breathing modes of the Cu-O₆ complex, with an important implication of the apical oxygen. Here we mention these modes for the most known HTSC. For example in La_2CuO_4 , optical measurements have determined the oxygen breathing mode frequencies⁴⁰ in the range 400-640 cm^{-1} ; G. Deutscher et al²⁶

have measured the phonon spectrum by point contact spectroscopy and they found many involved phonons between 160 cm^{-1} and 480 cm^{-1} . For $\text{YBa}_2\text{Cu}_3\text{O}_7$ ⁴¹, these important modes are in the range 340-610 cm^{-1} . In this compound, the 340 cm^{-1} mode frequency seems to play a particular role⁴². Then, in $\text{Bi}_2\text{Sr}_2\text{CaCu}_2\text{O}_8$, the mode frequencies⁴³ assigned to the axial phonon ($\parallel c$) and involved in an electron-phonon interaction are 445 cm^{-1} and 594 cm^{-1} ; other phonons seem to play an important role, like the 587.2 cm^{-1} mode frequency due to the phonons in the Bi-O plane and the 645.2 cm^{-1} , associated with those in the Cu-O plane⁴⁴.

Moreover, we know that the mode frequencies are screened by the carriers and renormalised in the interaction. Therefore, we have chosen for $\hbar\omega_0$ in our calculations, an arbitrary average phonon of 480 cm^{-1} or 60 meV, which is in the range 160-640 cm^{-1} .

We have tried other values for $\hbar\omega_0$ of the same order of magnitude, and we have observed no significant change in the results. This observation confirms the anomalous isotope effect already observed and explained in these materials².

The numerical results are presented in table I : we see that there is a good agreement between our computation and the experimental values. The set of parameters ($t = 0.20 \text{ eV}$, $\hbar\omega_0 = 60 \text{ meV}$) has been chosen on figure 7-2, where we plot the gap $\Delta(\Phi)$ as a function of the angular coordinate Φ , using the first two terms in the Fourier expansion

$$\Delta(\Phi) = \Delta_0 + \Delta_1 \cos 4\Phi$$

with $\Delta_0 = 14 \text{ meV}$ and $\Delta_1 = 8 \text{ meV}$, for $T_c = 88.5 \text{ K}$ (solid line); and with $\Delta_0 = 12.5 \text{ meV}$ and $\Delta_1 = 7.5 \text{ meV}$, for $T_c = 78.5 \text{ K}$ (dashed line).

The black dots represent the experimental values for several samples as published by Shen et al³⁶, and Hong Ding et al⁴. The agreement seems very good considering the experimental accuracy of ARPES measurements and the approximations made in our theory. Figure 7-3 gives the variation, with temperature T , of the average gap Δ_0 (14 meV at $T = 0 \text{ K}$), the maximum gap Δ_{\max} (22 meV at $T = 0 \text{ K}$), the minimum gap Δ_{\min} (6 meV at $T = 0 \text{ K}$). Here we obtain a T_c value of 88.5 K, close to the experimental one.

We find that $\frac{2\Delta_0}{k_B T_c} = 3.7$ (very close to the BCS value), $\frac{2\Delta_{\max}}{k_B T_c} = 5.8$ and $\frac{2\Delta_{\min}}{k_B T_c} = 1.6$

This explains perhaps the different values observed in various experiments.

Table I : Several sets of parameters for the calculated gap, for $\hbar\omega_0 = 60$ meV and with two choices for the transfer integral : $t = 0.20$ eV (Table I-a) and $t = 0.25$ eV (Table I-b).

TABLE I-a

q_0^a	$\hbar\omega_0=60\text{meV}$ λ_{eff}	$t=0,20$ eV Δ_A meV	Δ_B meV	Δ_0 meV	T_c (K)	$2 \Delta_0 / k_B T_c$
0.18	0.570	22	6	14.0	88.5	3.7
0.12	0.785	22	5	13.5	84.4	3.7
0.13	0.370	20	7	13.5	84.5	3.7
0.08	1.100	22	4	13.0	81.5	3.7
0.23	0.450	20	6	13.0	82.0	3.7
0.05	1.670	22	3	12.5	78.5	3.7
0.15	0.620	20	5	12.5	78.5	3.7

TABLE I-b

q_0^a	$\hbar\omega_0=60\text{meV}$ λ_{eff}	$t=0,25$ eV Δ_A meV	Δ_B meV	Δ_0 meV	T_c (K)	$2 \Delta_0 / k_B T_c$
0.190	0.50	22	6	14.0	87.5	3.7
0.130	0.67	22	5	13.5	84.5	3.7
0.350	0.31	20	7	13.5	85.0	3.7
0.085	0.94	22	4	13.0	81.5	3.7
0.250	0.39	20	6	13.0	82.0	3.7
0.045	1.60	22	3	12.5	77.5	3.7
0.165	0.53	20	5	12.5	78.5	3.7

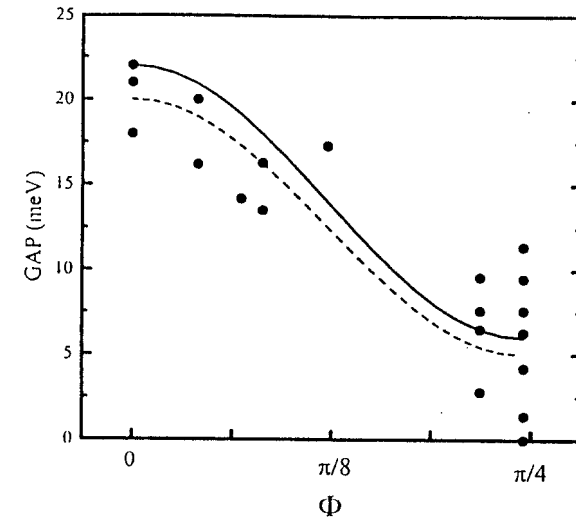


Fig. 7-2 : Angle-dependent calculated gap $\Delta(\Phi)$ for two sets of parameters : $\Delta_0 = 14$ meV, $\Delta_1 = 8$ meV, for $T_c = 88.5$ K (solid line), and $\Delta_0 = 12.5$ meV, $\Delta_1 = 7.5$ meV, for $T_c = 78.5$ K (dashed line) ; experimental values from references [4] and [34] (black dots).

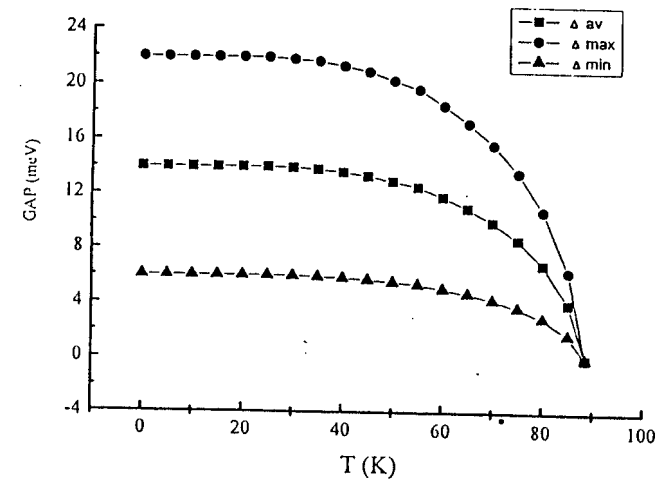


Fig. 7-3 : Temperature-dependent maximum (full circle), average (full square) and minimum (full triangle) gaps; for $T = 0$ K, $\Delta_{\text{av}} = \Delta_0 = 14$ meV, $\Delta_1 = 8$ meV, and for a $T_c = 88.5$ K.

8. Conclusion

We have calculated different properties of high T_c cuprates using an itinerant electron model in a two dimensional periodic potential leading to van Hove singularities. We assume, in addition, that the v.H.s. lie close to the Fermi level. This last assumption has been confirmed by many photoemission (ARPES) experiments.

This enables us to predict high T_c , an anomalous isotope effect, a very short coherence length, a Pauli susceptibility varying as $\ln(1/T)$ and an anisotropic gap. We have also taken into account the Coulomb repulsion and have shown that we get an important renormalization effect, μ^* being of the order of $\mu/4$.

As regards the order parameter, we find for Bi 2212 for example, a minimum gap of 6 ± 2 meV and a maximum gap of 20 ± 3 meV. We use only experimentally determined parameters in our calculation, except for a rather low isotropic value of q_0 that is essential to obtain a large anisotropy. In these materials which are intermediate between metals and ionic crystals, the Debye screening radius is not of atomic size as in good metals, but much larger³⁵. The two dimensional character of these compounds is also responsible for a poor screening. The mobile carriers move in planes, and so are unable to screen out completely the electric field in the third dimension.

The gap values obtained theoretically agree very well with the values determined by various experiments such as ARPES and tunnel effect. We thus obtain an "extended s-wave" gap⁴⁵ and not a d-wave pair function. The order parameter is never negative in our model. A.A. Abrikosov⁴⁶ has shown however that if a short range repulsive interaction (which can represent either some part of the Hubbard repulsion at the copper sites or the interaction mediated by spin fluctuations) is added, then the order parameter can vary in sign and become negative at points of the Fermi surface distant from the singularity. The anisotropy of the dielectric constant should be taken into account to obtain a more detailed description of the material.

Such an approach may reconcile all the observations leading sometimes to s-wave and other times to d-wave symmetry of the order parameter.

9. References

1. D. Pines. *Physica C* **235-240** (1994) 113.
2. J. Labbé, J. Bok, *Europhysics Letters* **3** (1987) 1225.
3. Z. X. Shen, W.E. Spicer, D.M. King, D.S. Dessau, B.O. Wells, *Science* **267** (1995) 343.
4. Hong Ding, J. C. Campuzano, K. Gofron, C. Gu, R. Liu, B. W. Veal and G. Jennings. *Phys. Rev. B* **50** (1994) 1333.
5. Jian Ma, C. Quitmann, R.J. Kelley, P. Alméras, H. Berger, G. Margaritondoni, M. Onellion. *Phys. Rev. B* **51**, (1995) 3832.
6. H. Krakauer, W. E. Pickett, R. E. Cohen. *Phys. Rev. B* **47** (1993) 1002.
7. J. Rossat-Mignot et al. *Physica B* **199-200** (1994) 281.
8. L. P. Regnault et al. *Physica C* **235-240** (1994) 59.
9. J. L. Tallon. Proceedings of the "Workshop on high temperature superconductivity". Miami, 5-11 January 1995. To be published in *Journal of Superconductivity*.
10. L. van Hove, *Phys. Rev.* **89** (1953) 1189.
11. L. Force et J. Bok, *Solid State Comm.* **85** (1993) 975.
12. D.L. Novikov, V.A. Gubanov et A.J. Freeman, *Physica C* **210** (1993) 301.
13. M. Hirao, T. Uda et Y. Marayama, *Physica C* **195** (1992) 230.
14. D.L. Novikov and A.J. Freeman, *Physica C* **3** (1993) 4.
15. K. Gofron, J.C. Campuzano, *J. Phys. Chem. Sol.* **53** (1992) 1577.
16. D. S. Dessau, Z. X. Shen, D. M. King, D. S. Marshall, L. W. Lombardo, P.H. Dickinson, J. DiCarlo, C. H. Park, A. G. Loeser, A. Kapitulnik and W.E. Spicer. *Phys. Rev. Lett.* **71** (1993) 2781.
17. D.Y. Xing, M. Liu et C.D. Dong, *Phys. Rev. Lett.* **68** (1192) 1090.
18. Y. Koike et al, *Physica C* **159** (1989) 105.
19. C.C. Tsuei, D.M. Newns, C.C. Chi et P.C. Pattnaik, *Phys. Rev. Lett.* **65** (1990) 2724. D.M. Newns, C.C. Tsuei, P.C. Pattnaik and C.L. Kane, *Comments Cond. Mat. Physics* **15**, 273 (1992).
20. G.G. Olson et al, *Phys. Rev. B* **42** (1990) 381.
21. Z. Schlesinger et al. *Phys. Rev. Lett.* **67** (1991) 1657.
22. Y. Kubo et al. *Phys. Rev. B* **43** (1991) 7875.
23. P. W. Anderson and P. Morel. *Phys. Rev.* **125** (1962) 4.
24. M.L. Cohen and P.W. Anderson in *Superconductivity in d- and f-Band Metals*, ed. D.H. Douglass (AIP, New York, 1972)
25. V. Ginzburg. *Contemporary Physics* **33** (1992) 15.
26. G. Deutscher, N. Hass, Y. Yagil, A. Revcolevschi, and G. Dhalenne. *J. Supercond.* **7** (1994) 371.
27. G. Deutscher, P. Nozières. *Phys. Rev. B* **50** (1994) 13557.
28. J. Bok and J. Labbé. *C.R. Acad. Sci.* **305** (1987), 555.
29. K. Sauv, M. Nicolas and J. Conard. *Physica C* **223** (1994) 145.
30. K. Sauv, J. Conard and M. Nicolas. *Physica C* **235-240** (1994) 1731.
31. J. Bok, J. Bouvier. *Physica C* **244** (1995) 357.
32. A. Bansil, M. Lindros, K. Gofron and J.C. Campuzano. *J. Phys. Chem. Solids* **54** (1993) 1185.
33. J. C. Carter, L. H. Bennett, D. J. Kahan, *Metallic shifts in NMR, Progress in Materials Science*, vol **20** (Pergamon, Oxford, 1977).
34. J. Bardeen, L. N. Cooper and J. R. Schrieffer. *Phys. Rev.* **108** (1957) 1175.
35. A.A. Abrikosov. *Physica C* **222** (1994) 191.
36. Z. X. Shen, D.S. Dessau, B. O. Wells, D. M. King, W. E. Spicer, A. J. Arko, D. Marshall, L. W. Lombardo, A. Kapitulnik, P. Dickinson, S. Doniach, J. DiCarlo, A. G. Loeser and C.H. Park. *Phys. Rev. Lett.* **70** (1993) 1553.
37. B. A. Aminov, M. A. Hein, G. Muller, H. Piel, D. Wehler. *J. Supercond.* **7** (1994) 361.

38. Ch. Renner and O. Fischer. *Phys. Rev B* **51** (1995) 9208.
39. D. S. Dessau, Z. X. Shen, D. M. King, D. S. Marshall, L. W. Lombardo, P.H. Dickinson, J. DiCarlo, C. H. Park, A. G. Loeser, A. Kapitulnik and W.E. Spicer. *Phys. Rev. Lett.* **71** (1993) 2781.
40. C. Thomsen and M. Cardona in "*Physical Properties of High Temperature Superconductors*" ed. D. M. Ginsberg (World Scientific, Singapore, 1989) pp 409-507.
41. I.I. Mazin et al, in "*Lattice Effects in High-Tc Superconductors*" ed. Y. Bar Yam, T. Egami, J. Mustre-de-Leon and A. R. Bishop (World Scientific, Singapore 1992). - C. Thomsen, M. Cardona, B. Friedl, C.O. Rodriguez, I. I. Mazin and O. K. Andersen. *Solid Stat. Comm.* **75** (1990) 219.
42. K. F. McCarty, J. Z. Liu, R. N. Shelton and R. N. Radousky. *Phys. Rev. B* **41** (1990) 8792 - L. V. Gaparov, V. D. Kulubovskii, O.V. Misochka and V. B. Timofeev. *Physica C* **157** (1989) 341. - R. M. Macfarlane, Hal Rosen and H. Seki. *Solid Stat. Comm.* **63** (1987) 831.
43. G. Ruani, C. Taliani, R. Zambeni, V. M. Burlakov and V. N. Denisov. *Solid Stat. Comm.* **78** (1991) 979.
44. H. C. Gupta. *Physica C* **157** (1989) 257.
45. J. Bouvier and J. Bok. *Physica C* **249** (1995) 17-22
46. A.A. Abrikosov. *Physica C* **244** (1995) 243.